Origin of noise in AlGaN/GaN heterostructures in the range of 10–100 MHz

S. A. Vitusevich,[a] S. V. Danylyuk, A. M. Kurakin, N. Klein, and A. Offenhäusser
Institut für Schichten und Grenzfächen and Center of Nanoelectronic Systems for Information Technology (CNI), Forschungszentrum Jülich, Jülich D-52425, Germany

M. V. Petrychuk
Taras Shevchenko National University, Kiev 01033, Ukraine

A. E. Belyaev
V. Lashkaryov Institute of Semiconductor Physics, NASU, Kiev 03028, Ukraine

(Received 11 July 2005; accepted 27 February 2006; published online 10 April 2006)

We report on the noise origin in AlGaN/GaN heterostructures for the frequency range of 10–100 MHz. High electron mobility transistor heterostructures were designed for high-power and high-frequency application and grown on SiC substrates. The structures were patterned with Ohmic transmission line model (5, 10, 15, 20, and 25 micrometer working distances) contacts and were analyzed using *I-V* characteristics and noise figure measurements. Different possible mechanisms of noise origin were considered and investigated in detail. The results of our analysis show that the thermal noise and hot carrier noise play a minor role in the structure in the investigated frequency range. At the same time, a dominant generation-recombination (*G-R*) noise is revealed. Moreover, two different components of *G-R* noise are found demonstrating different temperature dependences and as a result different physical origins of the noise are established. A detailed analysis of potential profiles of the structure calculated self-consistently for several voltages allows us to propose a physical model for the observed noise behavior. The fluctuations of electron concentration on the first quantum level of the quantum well and the scattering of the electrons in the barrier layer play a definite role in the noise phenomena. © *2006 American Institute of Physics*.
[DOI: 10.1063/1.2188048]

I. INTRODUCTION

AlGaN/GaN high electron mobility transistors (HEMTs) and amplifiers based on them are important components of high-frequency communication systems, including different kinds of oscillators.[1] For emerging signal-processing applications, the properties of noise characteristics play a critical role. While a number of studies have been made on predicting the noise origin in oscillators, the subject is still under hot discussion[2] due to strong nonlinear operation conditions in the oscillator circuit. The investigation of fluctuation phenomena of the HEMT structure in a wide range of applied electrical fields is an important issue because its noise is up-converted to high-frequency noise in the oscillator circuit,[3] and especially the MHz frequency range plays a crucial role. This frequency region (where $1/f$ noise decreases to the level of white noise) is an intermediate one. The lower the level of noise in this region, the lower and the narrower is up-converted high-frequency band noise. Noise reduction in this region will allow the density and rate of transmitted information in communication systems to be increased. III-nitride materials and heterostructures are excellent candidates for high-power, and therefore for extremely low-phase noise, high-frequency oscillator development.[4] Additional noise reduction and increasing stability and reliability are expected after characterization of trap centers, control of the trap-related effects, and structure passivation. Investigations of low-frequency fluctuations have proven to be useful for studying "slow" fluctuations at low electric fields (E), while the study of intermediate-frequency and high-frequency range fluctuations with increasing E and "fast" process phenomena (where hot electron effects, energy, and impulse relaxation mechanisms become essential) is more important for various applications. The optimal value of the minimum noise in field effect transistors (FETs) is usually obtained with a relatively low drain and gate voltage,[5] while high operation voltages are desirable for power applications. One of the reasons for high-frequency noise in FETs proposed in Ref. 6 is the hot carrier noise. In this case, the carrier lifetime and the noise level of the device are determined by interface states, introduced by hot carriers. The authors found that the presence of interface states decreases the channel conductance and high-frequency thermal current noise, and at the same time increases the induced gate current noise.

The effect of surface passivation and surface states on high-frequency noise performance of FET devices[7] was investigated by using a SiN passivation layer. However, in spite of the expected noise decrease, increasing noise was registered mainly due to the decrease of associated power gain, attributed to increased gate-source and gate-drain capacitances.

Detailed analysis by Pantisano and Cheng[8] of the FET high-frequency noise (1–2.5 GHz) as a function of degradation induced by electrical stress allows them to conclude that

[a]Author to whom correspondence should be addressed; on leave from Institute of Semiconductor Physics, NASU, 03028 Kiev, Ukraine electronic mail: s.vitusevich@fz-juelich.de

the physical origin of FET noise differs from that following from the usually accepted physical models of thermal noise and is due to previously unaccounted flicker noise at microwave (MW) frequencies. The FET MW noise study revealed a defect-related (flicker) origin of the noise in the FET. It was demonstrated that in order to contribute to the high-frequency noise, the traps must be very close to the interface. In this case, tunnelling can be very efficient and the minimum time constant for the charge exchange must be much shorter than 10 ns. Therefore, the authors provide evidence that the high-frequency noise of the FET should not be thermal.

We report the results of investigations of voltage fluctuations in AlGaN/GaN heterostructures in the frequency range from 10 to 100 MHz in a wide range of applied biases. For detailed analysis of the noise origin we used two equivalent approaches: expressing noise through noise temperature as well as through the resistance fluctuation model. Additionally, self-consistently calculated potential profiles of the structure at different voltages were analyzed.

II. EXPERIMENTAL DETAILS

All measurements were performed at room temperature. The structures were grown by metal-organic chemical-vapor deposition (MOCVD) on SiC substrate. A two-dimensional electron gas (2DEG) was formed by undoped AlGaN/GaN layers. A detailed description of layer structure can be found elsewhere.[9] As the object of investigation, a set of Ohmic contacts in the form of transmission line model (TLM) structures was used with a channel length between the contacts of $L=5$, 10, 15, 20, and 25 μm. The noise was measured in a so-called "longitudinal" configuration, where the same contacts are used for applying current and measuring voltage fluctuations. The noise and high-frequency conductivity were measured with a Hewlett-Packard noise figure meter HP 8970B.

Typical current-voltage dependences of the TLM structures are shown in Fig. 1(a). The dependences are linear up to bias voltages $U \approx 1-2$ V (depending on length of the structure). At higher voltages the current growth decreases and eventually saturates. As it was also shown,[10] the dependence of the relative change of resistance on dissipated power $P=IU$ is linear [Fig. 1(b)] and coincides for samples of different lengths. Assuming that the increase of temperature is proportional to the dissipated power we can conclude that the change of resistance of the sample is proportional to the change of temperature. This fact will be used in our later analysis.

III. RESULTS AND DISCUSSION

Spectral density of voltage fluctuations S'_V was extracted from the measured noise figure using equation

$$F = 10 \log \frac{S'_V + S_{V0}}{S_{V0}}, \tag{1}$$

where $S_{V0}=4kT(50)$ is the thermal noise of the 50 Ω impedance waveguide, k is the Boltzmann constant, and T is the temperature. It should be noted that the noise of the noise figure meter device is excluded. Typical voltage noise results measured at frequency $f=90$ MHz for HEMT structure patterned with TLM contacts of different lengths from 5 to 25 μm versus applied voltage are shown in Fig. 2. The observed noise behavior correlates with the nonlinearity of the current-voltage characteristics.

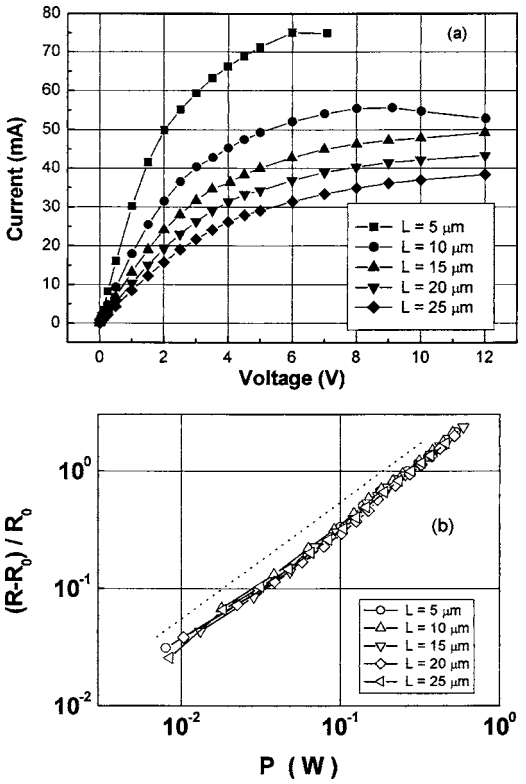

FIG. 1. (a) Current-voltage characteristics for the devices with a channel width of 100 μm and different channel lengths (shown in inset to the figure). (b) The relative change of resistance of TLM structures of the samples of different lengths measured as a function of dissipated power. Dashed line shows approximation slope.

To analyze the obtained noise results we considered three possible mechanisms of noise origin. Noise in the range from 10 to 100 MHz can contain equilibrium thermal (Nyquist) noise. It may also contain diffusive noise of hot electrons and excessive current noise, caused by generation-recombination processes. Below we consider each of the above-mentioned mechanisms in detail.

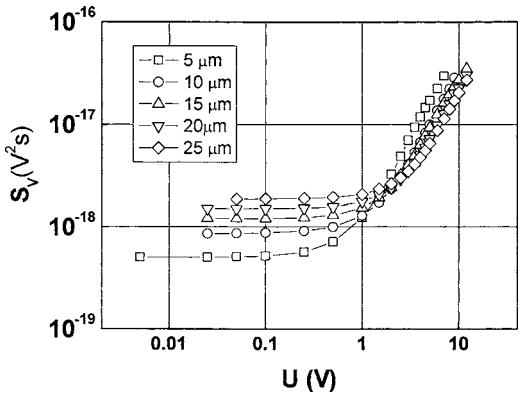

FIG. 2. Voltage noise spectral density measured at frequency $f=90$ MHz for TLM structures of different lengths vs applied voltage.

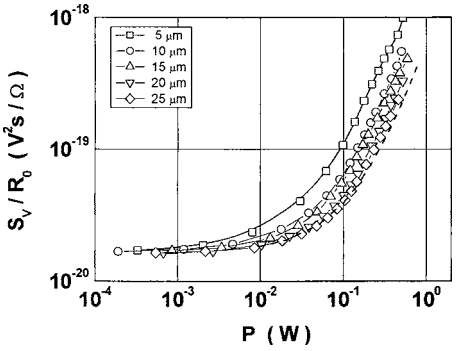

FIG. 3. Spectral density of noise fluctuations as a function of dissipated power, measured for samples of different lengths. Dashed curve corresponds to the theoretical curve according to Eq. (6) for the sample with a length of 25 μm.

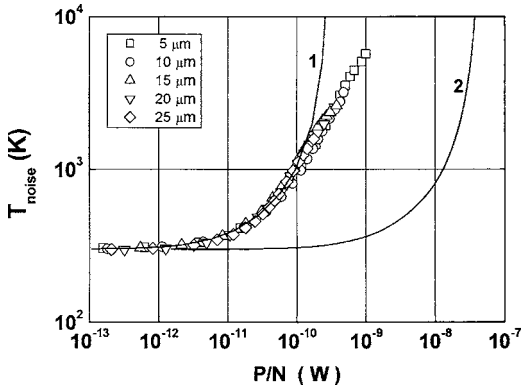

FIG. 4. Noise temperature dependence on dissipated power per one electron measured for samples of different lengths. Theoretical dependences calculated according to Eq. (7) calculated for $\tau_{ph}=50$ ns (curve 1) and $\tau_{ph}=350$ fs (curve 2) are shown by lines.

A. Thermal noise

The origin of the observed noise as a thermal noise will be discussed first. For the investigated voltage range, we consider that the shape of the electron distribution function does not change under applied biases. In this case, the temperature of the two-dimensional electron gas coincides with the lattice temperature, and the thermal noise spectral density is determined by the formula

$$S_V = 4kT\,\mathrm{Re}(Z), \tag{2}$$

where Z is full impedance of the object. The resistance of the sample in the case of self-heating can be determined as

$$R = R_0 + \Delta R, \tag{3}$$

where R_0 is the resistance without self-heating effect, and ΔR is the resistance deviation due to heating effect. Taking into account the linear dependence of the relative change of the resistance versus dissipated power, the resistance and the temperature of the sample can be described as

$$R = R_0 + k_1 P, T = T_0 + k_2 P, \tag{4}$$

where k_1 and k_2 are constants. Then the thermal noise can be written as

$$S_V = 4k(T_0 + k_2 P)(R_0 + k_1 P). \tag{5}$$

The equation after normalization to R_0 (obtained by extrapolation of R to $V=0$) will be represented in the following form:

$$\frac{S_V}{R_0} = 4k\left[T_0 + \left(\frac{k_1}{R_0}T_0 + k_2\right)P + \frac{k_1}{R_0}k_2 P^2\right]. \tag{6}$$

The value of k_1/R_0 equal to 3.67 W^{-1} is the same for all samples due to the coincidence of the curves shown in Fig. 1(b), corresponding to the samples of different lengths. According to the Eq. (6), $S_V(P)$ contains three terms: constant level term $S_{V0}=4kT_0R_0$, linear term, and term with quadratic versus power dependence. Figure 3 shows the theoretical dependence (6) calculated for the sample with a length of $L=25$ μm and the experimentally obtained relative noise increase as a function of the power for a frequency of $f=90$ MHz. From the coincidence of the fitting curve to the experimental data the coefficient k_2 is extracted equal to $k_2=2200$ K/W.

As can be seen, even if we assume that dissipated power is about 1 W, then the overheating value is $\Delta T=2200$ K (which is definitely much larger than any experimental evaluations), the value of the measured noise is still higher than the calculated noise. Moreover, the experimental dependences for samples of different lengths do not coincide as should follow from Eq. (6). Therefore, we can conclude that the observed noise cannot be the thermal noise.

B. Hot carrier noise

Let us now analyze the results within the model of diffusive hot electron noise, driven by the scattering of hot electrons on phonons.[11] For this we shall represent our measured noise in terms of noise temperature (experimental points in Fig. 4) and build the dependence of the noise on power applied to one electron. In the same coordinates we shall plot the value of hot electron noise, calculated with the empirical formula[11] that takes into account phonon scattering,

$$P_s = \Delta\varepsilon/\tau_{ph}\{\exp(-\Delta\varepsilon/kT_n) + [\exp(-\Delta\varepsilon/kT_n) - 1]/[\exp(\Delta\varepsilon/kT_L) - 1]\}, \tag{7}$$

where $\Delta\varepsilon=0.09$ eV is the energy of the optical phonon, $T_L=300$ K is the lattice temperature, T_n is the noise temperature, and P_s is the dissipated power per one electron. Curve 2 corresponds to the typical value of phonon time $\tau_{ph}=350$ fs;[12] curve 1, which partially coincides with the experimental points, corresponds to $\tau_{ph}=50$ ns, which is much higher than the value commonly used for GaN-based structures. Consequently, the hot electron noise cannot explain the observed results either.

C. Generation-recombination noise

Let us now consider the third possibility: measured noise is generation-recombination (G-R) noise. This is determined by the following formula:[13]

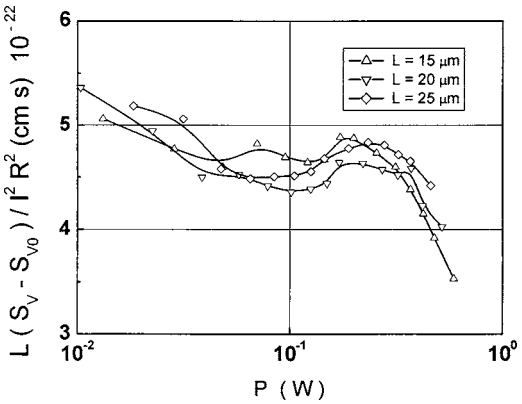

FIG. 5. Dependence of normalized noise of samples of different lengths on dissipated power at $f=90$ MHz.

$$S_l = 4\frac{\overline{\Delta N^2}}{N^2}\frac{I^2\tau}{1+(\omega\tau)^2}, \tag{8}$$

where $S_I=S_V/R^2$ is the spectral density of current fluctuations, N is the mean value of full number of electrons in a sample, $\overline{\Delta N^2}$ is the mean square value of deviation of electron number from its mean value, ω is the frequency, and τ is the time constant of *G-R* process. The value $\overline{\Delta N^2}/N=g$ depends only on the statistics of electrons and not on N. Let us assume that the investigated frequency $f=90$ MHz lies within a region where $\omega\tau \ll 1$. Then expression (8) can be written as

$$\frac{S_l N}{I^2} = 4g\tau. \tag{9}$$

The right side of (9) does not depend on sample size but can depend on temperature (dissipated power). Therefore we shall build a dependence of the left side of (9) on dissipated power, taking into account that a number of electrons N are proportional to length of a sample L. Since, as stated above, the temperature of the sample is determined solely by dissipated power, the curves obtained for different lengths should coincide (due to coincidence of corresponding resistance-power characteristics for different sample lengths).

As the thermal noise is always present at the nonzero temperature, we should subtract the value $S_{V0}=4kT_0R$ from the analyzed spectra. As a result we obtain dependence of value $L(S_V-S_{V0})/I^2R^2$ on dissipated power $P=UI$ (Fig. 5).

Additional thermal noise $S_{VT}=4k(T-T_0)R$ under condition $T-T_0=k_2P$ (as explained above) equals

$$S_{VT} = 4kk_2I^2R^2. \tag{10}$$

In the coordinates of Fig. 5

$$\frac{LS_{VT}}{I^2R^2} = 4kk_2L. \tag{11}$$

At $k_2=1200$ K/W (the extraction procedure for this coefficient will be described below) and $L=25$ μm, $4kk_2L=1.66\times10^{-22}$ cm s can be obtained. The value is much lower than the measured level of noise. At smaller lengths the value will only be lower, so that this additional thermal noise can be neglected.

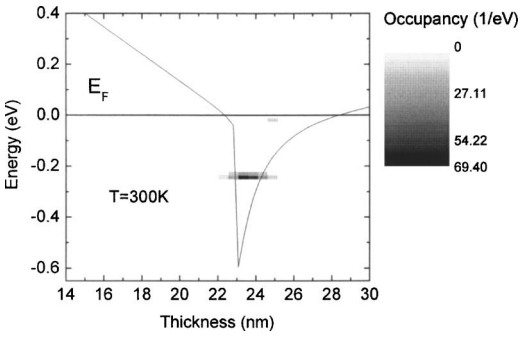

FIG. 6. Calculated local density of states and potential profile of the HEMT structure at $T=300$ K.

It is seen from Fig. 5 that not only do the curves for $L=25$, 20, and 15 μm coincide well at low power, but also the position and shape of the special feature observed at high power in the range from 0.1 to 0.6 W coincide with the maximum at $P\approx0.25$ W. This feature confirms our assumption of the *G-R* character of the observed noise.

Two kinds of transport mechanisms in two-dimensional electron channels may be responsible for generation-recombination noise. The first one is the electron redistribution due to the presence of more than one quantum level with different mobility. In this case, spontaneous transitions between the levels lead to fluctuations of the total conductance of the channel. This model was used in Ref. 14 to explain excessive noise at $f=10$ GHz. The second reason for the *G-R* noise can be the penetration of the 2D electron wave function to the barrier region of the structure, where the concentration of traps is generally higher. The mobility of these electrons is therefore reduced due to interaction with the traps.

To analyze the influence of the first suggested mechanism of *G-R* noise we self-consistently calculated the potential profile of the structure at different temperatures. The band diagram calculated for temperature $T=300$ K is shown in Fig. 6. The positions of the ground and first excited quantum levels in 2DEG relative to the Fermi energy calculated for different temperatures are shown in Fig. 7(a). It is interesting to note that at $T\approx600$ K the position of the first excited level coincides with the Fermi energy. According to the theory of *G-R* noise, the temperature dependence of Eq. (9) should have a maximum at this point. Indeed, in Fig. 5 we observe such a maximum at $W\approx0.25$ W, which allows us to ascribe this noise feature to the fluctuation of the number of electrons at the first excited quantum level. Now we can estimate the value of k_2: $k_2=\Delta T/P=300$ K/0.25 W $=1200$ K/W. This value is much smaller than $k_2=2200$ K/W used in our analysis of the influence of thermal noise (Fig. 3) and can serve as further evidence of the negligible role of equilibrium thermal noise in the total measured noise spectra.

To evaluate the role of the second reason mentioned above for excessive noise in the structure, we plotted electron density normalized to a maximum (in the ground level of 2DEG) as a function of coordinate x, perpendicular to the 2DEG layer [Fig. 7(b)]. Increasing the temperature leads to a rise of electron density within the barrier layer ($x<23$ nm).

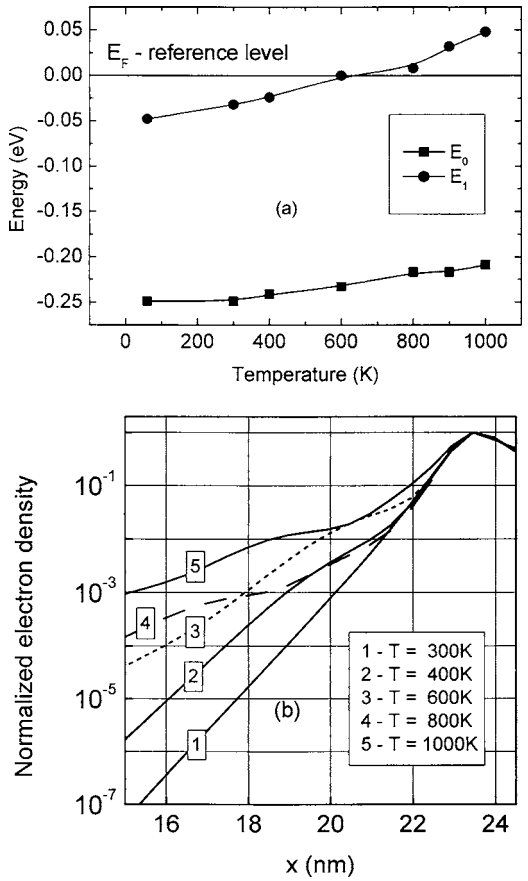

FIG. 7. Results of self-consistent calculation of Poisson and Schrödinger's equations. (a) Dependence of position of ground and first exited levels in 2DEG. (b) Distribution of density of 2DEG in the direction perpendicular to the interface at different temperatures. The interface position is at 23 nm in the calculation.

This rise should lead to an increasing number of electrons with lower mobility and, consequently, to an increase in the noise caused by an exchange between fast and slow electron populations. But, as is seen from Fig. 5, the total noise of the structure does not increase with temperature (dissipated power). Therefore this model cannot be used to explain the results of noise measurements at $f=90$ MHz.

A similar analysis was carried out for noise results obtained at 20 MHz frequency. The temperature dependence of Eq. (9) was also found to coincide for samples of different lengths [Fig. 8(a)], but in this case the character of the dependence differs from the results obtained at $f=90$ MHz.

Our analysis shows that the noise also has a generation-recombination character, but of different origin. The frequency dependence of noise measured at a dissipated power of 0.3 W [Fig. 8(b)] shows nonzero frequency slope, which can be analyzed as a spectrum combined from two noise components. The first one is a high-frequency component described above for $f=90$ MHz. The second one is at lower frequencies, with a corner frequency of around $f_0=50$ MHz, which corresponds to the time constant $\tau=3.2$ ns. This component can originate from the increase in the population of electrons in the barrier region of the structure with temperature [Fig. 7(b)]. This model can explain the effect of increasing noise at 20 MHz with a rise of dissipated power and, correspondingly, with an increase of temperature [Fig. 8(a)].

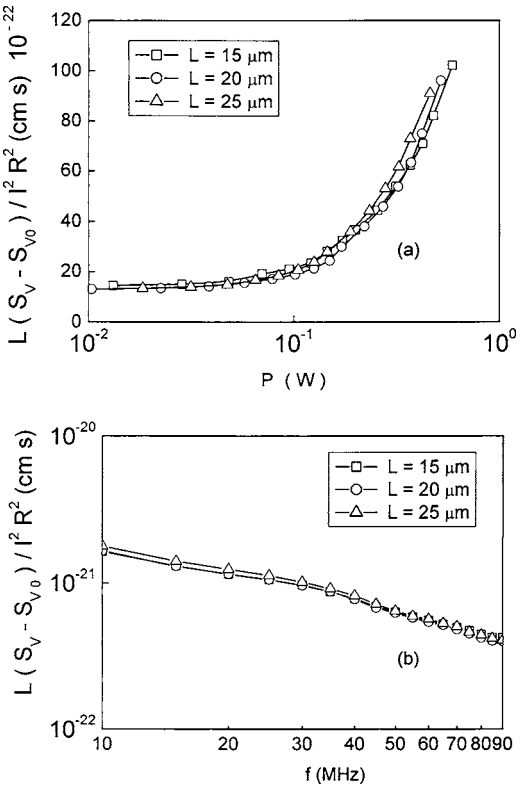

FIG. 8. (a) Dependence of normalized noise of samples of different lengths on dissipated power at $f=20$ MHz; (b) normalized noise spectra of TLM samples of different lengths measured at dissipated power $P=0.3$ W.

IV. CONCLUSIONS

The noise figure and the corresponding value of voltage noise fluctuations of AlGaN/GaN transistor heterostructures are analyzed in the important frequency range from 10 to 100 MHz for different applied biases. It was established that the observed noise cannot be thermal noise, because this would yield an extremely high overheating temperature, about 2200 K. Also hot carrier noise cannot explain the observed results, since in this case phonon lifetime should be very long, i.e., about 50 ns. At the same time, the results are very well described in the generation-recombination noise approach. Moreover, two independent components of the noise with different temperature behavior were observed and investigated. It was determined that the maximum observed in the temperature dependence of noise is caused by *G-R* fluctuations at points of coincidence of quantum level with Fermi energy. Therefore the noise, measured at $f=90$ MHz, originates from fluctuations of concentration at the first excited quantum level of 2DEG. Another *G-R* component was observed at lower frequencies with time constant $\tau=3.2$ ns. This demonstrates a different temperature dependence. The mechanism of the noise can be explained by increasing the penetration of electron wave functions into the barrier region with increase of self-heating.

ACKNOWLEDGMENT

This work is supported by the Deutsche Forschungsgemeinschaft (Project No. KL 1342).

[1]V. S. Kaper, R. M. Thompson, T. R. Prunty, and J. R. Shealy, IEEE Trans. Microwave Theory Tech. **53**, 55 (2005).
[2]J.-C. Nallatamby, M. Prigent, and J. Obregon, IEEE Trans. Microwave Theory Tech. **53**, 901 (2005).
[3]M. N. Tutt, D. Pavlidis, A. Khatibzadeh, and B. Bayraktaroglu, IEEE MTT-S Int. Microwave Symp. Dig. **2**, 727 (1992).
[4]S. V. Danylyuk, S. A. Vitusevich, V. Kaper, V. Tilak, N. Klein, L. F. Eastman, and J. R. Shealy, Phys. Status Solidi C **2**, 2615 (2005).
[5]H. Fakui, IEEE Trans. Electron Devices **ED-26**, 1032 (1979).
[6]H.-F. Tang, S.-L. Jang, and M.-H. Juang, Jpn. J. Appl. Phys., Part 1 **44**, 38 (2005).
[7]W. Lu, V. Kumar, R. Schwindt, E. Piner, and I. Adesida, Solid-State Electron. **46**, 1441 (2002).
[8]L. Pantisano and K. P. Cheung, J. Appl. Phys. **92**, 6679 (2002).
[9]S. A. Vitusevich *et al.*, Appl. Phys. Lett. **82**, 748 (2003).
[10]S. A. Vitusevich, S. V. Danyluk, N. Klein, M. V. Petrychuk, and A. E. Belyaev, J. Appl. Phys. **96**, 5625 (2004).
[11]J. Liberis and A. Matulionis, in *Noise and Fluctuations*, edited by J. Sikula (CNRL, Brno, 2003), pp. 241–246.
[12]A. Matulionis, J. Liberis, I. Matulioniene, M. Ramonas, L. F. Eastman, J. R. Shealy, V. Tilak, and A. Vertiatchikh, Phys. Rev. B **68**, 035338 (2003).
[13]A. Van der Ziel, *Noise in Solid State Devices and Circuits* (Wiley, New York, 1986), pp. 120–145.
[14]L. Ardaravicius, J. Liberis, A. Matulionis, L. F. Eastman, J. R. Shealy, and A. Vertiatchikh, Phys. Status Solidi A **201**, 203 (2004).